Drews *et al. Geotherm Energy* (2019) 7:3
https://doi.org/10.1186/s40517-019-0121-z

Geothermal Energy

RESEARCH

Predictability and controlling factors of overpressure in the North Alpine Foreland Basin, SE Germany: an interdisciplinary post-drill analysis of the Geretsried GEN-1 deep geothermal well

Michael C. Drews[1*], Peter Hofstetter[2], Kai Zosseder[2], Robert Straubinger[3], Andreas Gahr[3] and Harald Stollhofen[1]

*Correspondence:
michael.drews@fau.de
[1] Geozentrum Nordbayern, Friedrich-Alexander-University (FAU) Erlangen-Nuremberg, Schlossgarten 5, 91054 Erlangen, Germany
Full list of author information is available at the end of the article

Abstract

For the first time, drilling- and velocity based well analysis and 3D basin modeling were combined to test the predictability and controlling factors of overpressure in the North Alpine Foreland Basin in SE Germany. More specifically, the techniques were tested in the sub-regional context of the deep geothermal well Geretsried GEN-1 (TVD = 4852 m), located in the south of Munich. A 3D basin model based on a total of 20 wells was calibrated to the pressure distribution of four petroleum wells and tested against the Geretsried GEN-1 well. The results demonstrate that overpressure in the North Alpine Foreland Basin SE Germany can be predicted from a simple 3D basin model calibrated to a minimum number of wells. Thereby, disequilibrium compaction likely acts as the main overpressure mechanism in the study area, underpinned by significantly higher sedimentation rates at overpressured locations. 3D basin modeling also confirms the role of Upper Cretaceous shales, which, if present, serve as an important pressure barrier between the under- to normally pressured Jurassic and overpressured Cenozoic basin fill. In addition, overpressure magnitudes of the Chattian might be higher than previously expected. The results of this study have great impact on future drilling campaigns in the North Alpine Foreland Basin in SE Germany. Minimized non-productive time and drilling cost, improved well planning and increased safety are amongst the most important benefits of accurate pore pressure and overpressure prediction. The newly derived insights on the mechanisms of overpressure will greatly influence future geomechanical and tectonic studies, since pore pressure drives rock strength and principle stress magnitudes. Finally, the study is a great example for the importance of an interdisciplinary approach and the incorporation of geological conditions, when investigating drilling-related problems.

SpringerOpen

Introduction

Within any deep geothermal project, the highest risk is in the drilling, both economically and safety-wise (e.g. Stober and Bucher 2013). This especially applies to deep geothermal projects in basins with very deep target sections and with only a few wells being drilled per year, such as the North Alpine Foreland Basin in SE Germany. Quite often, the effective implementation and continuation of a deep geothermal project depend on the success of the first well drilled. Therefore, most deep geothermal projects are similar to classical wild cat exploration situations in basins such as the North Alpine Foreland Basin in SE Germany. Unexpected changes in pore pressure and subsurface stresses can lead to severe drilling problems such as influxes, kicks, blow-outs, drilling fluid losses, differential sticking, over-pulls, etc., which in the best case only delay drilling and cause economic burdens, but in the worst case endanger the continuation of the project or even pose a significant safety risk (Mouchet and Mitchell 1989). Therefore, careful well planning and adequate prediction of subsurface stresses and pressures are crucial for a successful completion of deep geothermal projects and deep drilling in general. This is particularly valid in overpressured basins (Mouchet and Mitchell 1989).

Overpressure is defined as the excess pressure above hydrostatic pore pressure given by a vertical depth, the formation water's density and the Earth's gravitational acceleration. Overpressure or pore pressure in general can be estimated from data sources such as geophysical well logs (Bowers 1995; Eaton 1972, 1975), seismic velocities derived from vertical seismic profiles, seismic surveys or sonic logs (Bowers 1995; Eaton 1972, 1975), drilling parameters (Mouchet and Mitchell 1989) and basin modeling (Bjørlykke et al. 2010; Darby et al. 1998; Karlsen and Skeie 2006; Mosca et al. 2018; Mudford et al. 1991; Peters et al. 2017; Satti et al. 2015). Origins of overpressure include disequilibrium compaction through retarded dewatering of pore fluids due to low-permeability barriers in the context of high sedimentation rates (Osborne and Swarbrick 1997; Swarbrick and Osborne 1998), fluid expansion through increased temperatures (Osborne and Swarbrick 1997; Swarbrick and Osborne 1998) or an increase in pore water caused by diagenesis (temperature-related hydroxide loss of clays (Osborne and Swarbrick 1997; Sargent et al. 2015; Swarbrick and Osborne 1998). Additional overpressure can be induced in extensive, laterally amalgamated and dipping sediments through lateral pressure transfer (Lupa et al. 2002; Yardley and Swarbrick 2000). Within the North Alpine Foreland Basin in SE Germany, overpressure is known to generally increase with burial depth from north to south and towards the Alps (Drews et al. 2018; Müller et al. 1988). Particularly to the south and east of Munich, overpressure can reach significant pressure gradients that translate into equivalent drilling fluid densities (mud weight) of 1.8 g/cm^3 or more (Drews et al. 2018; Müller et al. 1988).

Overpressure in the North Alpine Foreland Basin in SE Germany has been previously studied by Rizzi (1973), who demonstrated with two examples that overpressure can be estimated from geophysical well logs such as electrical resistivity and acoustic transit time (sonic log). Müller et al. (1988) and Müller and Nieberding (1996) were the first to study the regional distribution of maximum overpressure and its origin, based on a combination of maximum drilling mud weights and the structural interpretation of 2D seismic cross sections. They presented a regional map of maximum pore pressure gradients inferred from maximum drilling mud weights. Based on analysis of drilling data and velocity data, Drews et al. (2018) demonstrated that overpressure can be estimated with reasonable accuracy from seismic velocities of sonic logs and vertical seismic profiles. Drews et al. (2018) also were the first providing pore pressure gradient maps for all overpressured stratigraphic units present in the North Alpine Foreland Basin in SE Germany. However, previous works by Müller et al. (1988), Müller and Nieberding (1996) and Drews et al. (2018) were either based on drilling mud weight data and/or 1D velocity data of hydrocarbon wells, but did not incorporate 3D geologic models. Furthermore, these studies did not include any more recent deep geothermal wells from the North Alpine Foreland Basin in SE Germany, despite several deep geothermal wells have been drilled in the overpressured part of the basin during the past 2 decades.

A recent example of a deep geothermal exploration well in the overpressured section of the North Alpine Foreland Basin in SE Germany is given by the Geretsried Deep Geothermal Project, approximately 30 km SSE of Munich. In this study, the predictability and controlling factors of overpressure in the greater Geretsried area will be analyzed, combining drilling- and velocity data-based well analysis and pressure-centric 3D basin modeling. The results will be compared with pore pressure indicators from drilling data and a pore pressure estimate from vertical seismic profile data of the Geretsried GEN-1 well. The integration of these methods is the first of its kind in the North Alpine Foreland Basin in SE Germany, especially in the context of deep geothermal projects in South Germany. The results of this study are of great relevance to planning and drilling of future deep geothermal wells in the North Alpine Foreland Basin in SE Germany. Quantification of overpressure is also of great significance to geomechanical studies in the North Alpine Foreland Basin in SE Germany, e.g., considering the prediction of induced microseismicity caused by geothermal exploitation. In addition, the presented methodology and results will be a valuable reference case for other pore pressure studies to investigate overpressure distributions and mechanisms in sedimentary basins with a combination of different methods and from limited data sources.

Geological setting

The North Alpine Foreland Basin is a classical peripheral foreland basin. Its part in SE Germany stretches from Lake Constance in the west to the Austrian border in the east (Fig. 1). To the north, the extent of the North Alpine Foreland Basin in SE Germany is roughly outlined by the Danube River, and towards the south, it is bounded by the thrust-front of the Subalpine Molasse or Folded Molasse (Fig. 1). The wedge-shaped North Alpine Foreland Basin in SE Germany is filled with Cenozoic (Late Eocene to Late Miocene) sediments, which overlie Mesozoic pre-Molasse strata (Fig. 2). The target for the geothermal utilization is the highly permeable aquifer in the Upper Jurassic carbonate sediments, which are generally under- to normally pressured (Lemcke 1976).

The presence of overpressure in the North Alpine Foreland Basin in SE Germany has been attributed to disequilibrium compaction due to sedimentation rates exceeding dewatering rates of the buried fine-grained sediments (Drews et al. 2018; Müller et al. 1988). According to previous studies (Allen and Allen 2013; Zweigel 1998), peak sedimentation rates around 300 m/Ma occurred during Chattian and Aquitanian times. During the Cenozoic basin fill, fine-grained sediments forming shales and marls were primarily deposited during the high-stand phases in the Oligocene (Rupelian and

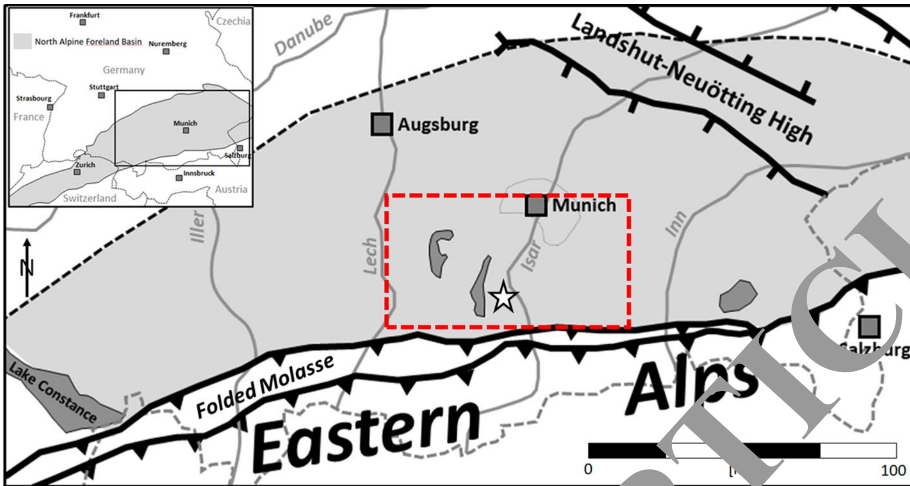

Fig. 1 Map of the North Alpine Foreland Basin in SE Germany (after Drews et al. 2018; Reinecker et al. 2010). The inset illustrates the location of the North Alpine Foreland Basin in SE-Germany. The gray area marks the outline of the North Alpine Foreland Basin in Germany and Western Switzerland. The study area is indicated by the red-dashed rectangle. The approximate location of the Geretsried GEN-1 well is highlighted by a white star

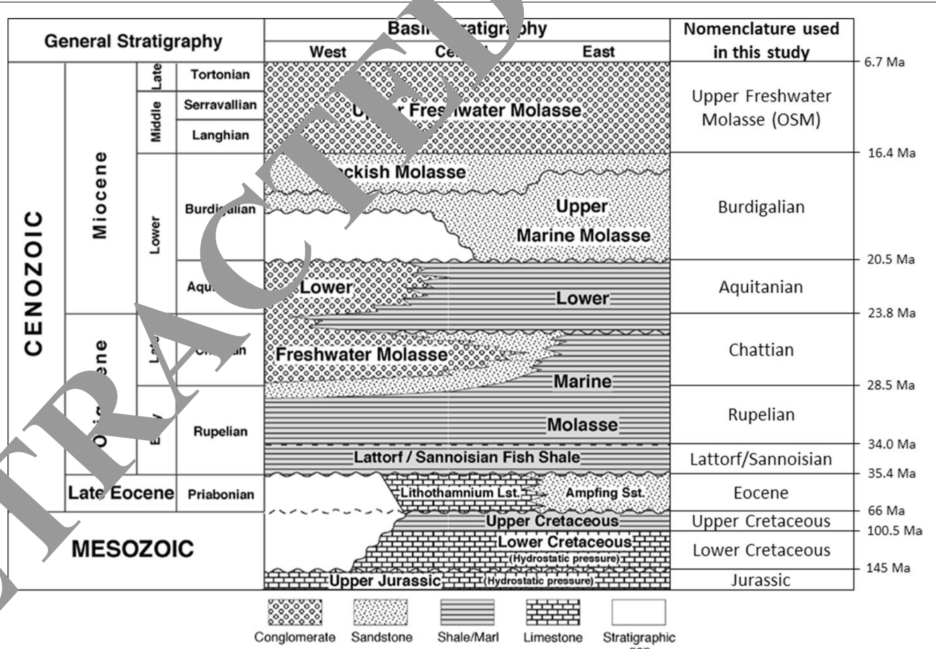

Fig. 2 Chronostratigraphic chart for the North Alpine Foreland Basin in SE Germany with nomenclature and geologic ages (after Drews et al. 2018). Geologic ages for Late Miocene-Rupelian, Sannoisian-Eocene and Mesozoic from Kuhlemann and Kempf (2002), Zweigel (1998) and Cohen et al. (2013), respectively

Chattian) and Lower Miocene (Aquitanian) (Fig. 2) (Kuhlemann and Kempf 2002). Overpressure in the Cenozoic section is usually found in Oligocene strata, in particular in the Lower Oligocene Lattorf/Sannoisian Fish Shale (Drews et al. 2018; Müller et al.

1988). In addition, Drews et al. (2018) interpreted the development of overpressure in Cenozoic sediments to be controlled by the presence of Upper Cretaceous shales retarding dewatering into the under- to normally pressured Upper Jurassic carbonate aquifer. Upper Cretaceous shales can also be significantly overpressured (Drews et al. 2018; Müller et al. 1988). However, Upper Cretaceous strata are not present in the west and northwest of the North Alpine Foreland Basin in SE Germany due to Paleocene/Eocene erosion (Bachmann et al. 1987) (Fig. 2). According to previous studies, Mid and Lower Jurassic sediments do not show any signs of overpressure (Drews et al. 2018).

Although the stress regime of the North Alpine Foreland Basin in SE Germany is controversially discussed (Drews et al. 2018; Greiner and Lohr 1980; Lohr 1978; Megies and Wassermann 2014; Müller and Nieberding 1996; Müller et al. 1988; Reinecker et al. 2010; Seithel et al. 2015; von Hartmann et al. 2016; Ziegler et al. 2016), Drews et al. (2018) showed that disequilibrium compaction with the assumption of vertical stress as a proxy for mean stress is a valid model to estimate pore pressure and overpressure from shale velocities in the North Alpine Foreland Basin in SE Germany.

Data and methods

The aim of this study is to (a) investigate how a combination of velocity-based pore pressure analysis, drilling data and basin modeling can be used to predict pore pressure in the North Alpine Foreland Basin in SE Germany and (b) what are the controlling geological factors on overpressure presence and generation in the greater area around the Geretsried GEN-1 well location. The 3D basin model is calibrated to velocity and drilling data-derived pore pressure profiles of wells in the greater Geretsried area. The calibration also serves the purpose of investigating overpressure mechanisms. The Geretsried GEN-1 well is not part of the calibration, but will serve as blind test. To do so, a 1D pore pressure extraction from the calibrated 3D basin model at the Geretsried GEN-1 well location is compared to the drilling history and drilling-related pore pressure indicators of the Geretsried GEN-1 well.

Drilling history and pore pressure indicators of the Geretsried GEN-1 well

The deep geothermal project "Geretsried Nord" was initiated by Enex Power Germany GmbH on the Wolfratshausen concession in September 2004. The Geretsried GEN-1 well was planned as a producer and was drilled approximately 5 km northwest of the city of Geretsried from mid-January 2013 to mid-July 2013. The well reached a total vertical depth of 4852 m (6036 m in measured depth). Despite excellent temperature conditions with a bottom-hole temperature of about 160 °C, the project was halted due to a lack of productivity in the targeted Upper Jurassic (Malm) carbonate aquifer. In 2017, due to a research project, a scientific sidetrack was drilled into a nearby fault zone in hopes of increased permeability, but it did not yield a sufficient increase in productivity. In true vertical depth TVD, the Geretsried GEN-1 well penetrated approximately 70 m of Quaternary sediments, 4162 m of Cenozoic deposits, 105 m of Cretaceous stratigraphy and 515 m of Upper Jurassic carbonates (Malm). The Geretsried GEN-1 well was drilled in five sections. Figure 3 is a graphical representation of the following description of the drilling history and pressure indicators of the Geretsried GEN-1 well.

In the first two sections low gas readings and a drilling mud weight of less than 1.2 g/cm^3 generally indicate balanced to overbalanced drilling and likely hydrostatic pressure conditions. However, within lower Aquitanian and Chattian shale sequences increased cavings, over-pulls and tight-hole sections were recorded, which might indicate underbalanced drilling and slightly elevated pore pressures. Accordingly, maximum total gas readings of 7.1% were detected in the sands of the Lower Chattian.

During drilling of the third section, the drilling mud weight was increased from 1.16 to 1.25 g/cm^3 followed by a water influx within Chattian/Rupelian sands of the so called Baustein Beds at 3285 m. Recorded shut-in pressures of 17.13 MPa and a drilling mud weight of 1.25 g/cm^3 indicate a formation pressure of 57.41 MPa or an equivalent mud weight of 1.78 g/cm^3. The drilling mud weight was, therefore, increased to 1.86 g/cm^3 until high total gas readings of up to 49% within the Lattorf/Sannoisian fish shales and possibly Eocene required a further mud weight increase to 1.94 g/cm^3, which finally stopped the increased gas readings. A formation pressure between 1.86 g/cm^3 and 1.94 g/cm^3 around 4115 m vertical depth is, therefore, likely. Subsequently, the section was cased with a 9 5/8″ string down to 4123-m vertical depth.

The followed section experienced high total gas readings and a small gas kick. Measured shut-in pressures within the Eocene Lithothamnium Limestone yielded formation pressures of 51.02 MPa or 1.26 g/cm^3 in equivalent mud weight. As a result, the drilling mud weight was increased from 1.24 to 1.31 g/cm^3, which stopped the gas influx.

The last section was drilled entirely within the Upper Jurassic carbonate aquifer (Malm) to a total depth of 4852 m vertical depth (6036 m measured depth) with a

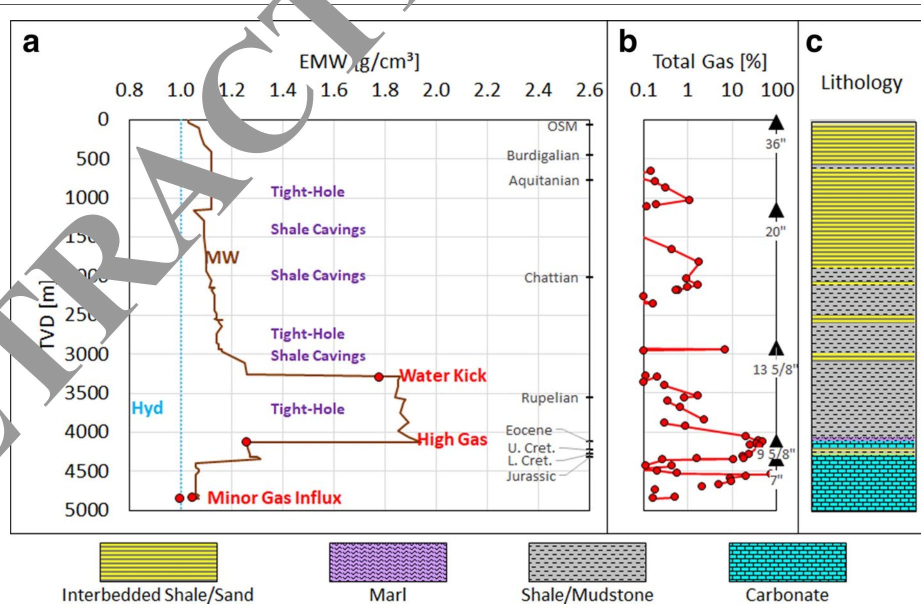

Fig. 3 Graphical representation of the drilling history and drilling-related pressure indicators of the Geretsried GEN-1 well. **a** Pressure in equivalent mud weight (EMW) in g/cm^3 vs. true vertical depth (TVD) with drilling mud weight MW (brown line), hydrostatic pressure Hyd (blue-dotted line), influx events (red dots and annotations), other overpressure indications (purple annotations) and stratigraphic tops. **b** Total gas readings while drilling on a logarithmic scale in percent (red lines and dots) and casing points (black triangles). **c** Simplified lithological profile based on cutting descriptions from the geological well report (legend on the bottom provides key for lithotypes)

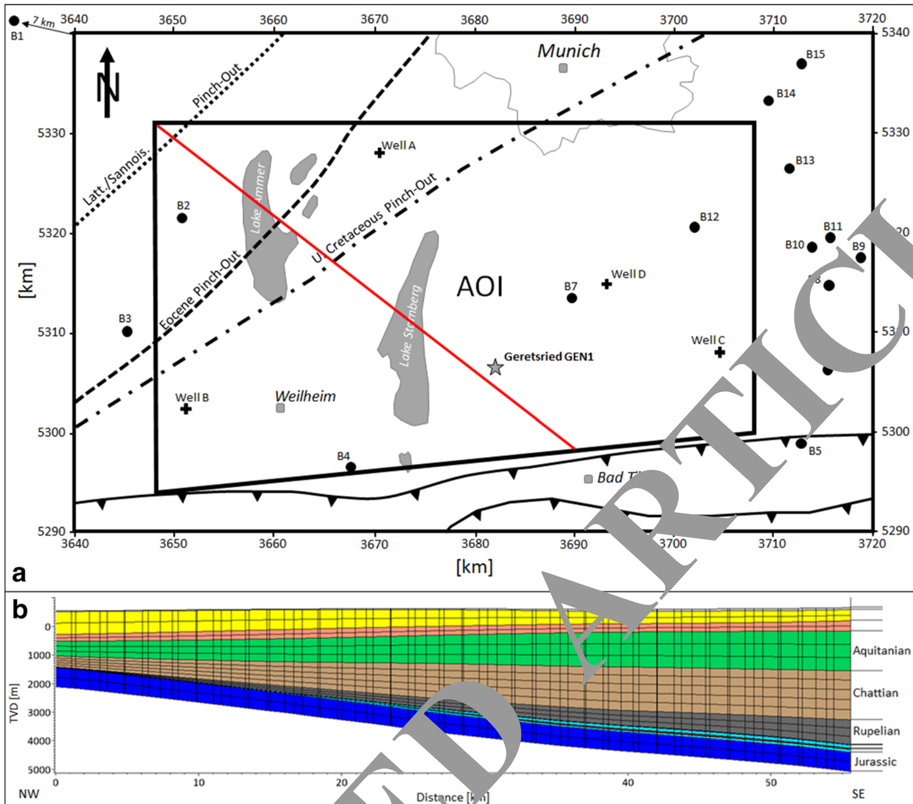

Fig. 4 Study area, basin model set-up and locations of used wells. **a** Study area and extent of 3D basin model with used wells and stratigraphic boundaries. The Geretsried GEN-1 drill site is marked with a gray star, the calibration wells A–D are marked with black crosses, while black dots indicate additional wells (B1–B15) used to constrain the 3D basin model. One well is outside of the map area and was used to constrain the extent of the Lattorf/Sannoisian. The map coincides with the extent of the full basin model, which has been reduced to an area of interest (AOI, marked by the black lined polygon) after simulation. According to the used well data, pinch-outs towards the north western part of the study area have been incorporated into the 3D basin model for Upper Cretaceous (dashed–dotted line), Eocene (dashed line) and Lattorf/Sannoisian (dotted line). The red line marks cross section represented in **b**. **b** NW–SE cross section through the basin model showing the individual layers, sublayers and incorporation of pinch-outs. Vertical scale in true vertical depth (TVD) in meters. The section is vertically exaggerated by a factor of 2

maximum drilling mud weight of 1.07 g/cm^3. However, high gas readings within the Upper Jurassic of up to 73% indicate underbalanced drilling and likely an Upper Jurassic aquifer, which is slightly overpressured and not as hydraulically active as described in other parts of the North Alpine Foreland Basin in SE Germany (c.f. Lemcke 1976). These observations fit with the low productivity rates found in the Geretsried GEN-1 well.

Study area and well data

The study area extends over an area of c. 80 × 50 km and is roughly centered by the Geretsried GEN-1 drill site approximately 30 km south of Munich (Fig. 4). The study area includes closer studied wells in the north (Well A), west (Well B), east (Well C) and northeast (Well D) of the Geretsried GEN-1 drill site (Fig. 4). Velocity and drilling data of these four wells have been studied in more detail to provide pressure calibration

Table 1 Well data used in this study

Well name	Drilling data	Velocity data	Geological data
Geretsried GEN-1	Drilling mud weight, gas readings, kicks, drilling reports, casing shoe points	Vertical seismic profile (data missing in Rupelian section)	Well tops, cutting descriptions
Well A	Drilling mud weight (log headers), casing shoe points	Vertical seismic profile, sonic log	Well tops, cutting descriptions
Well B	Drilling mud weight (log headers), gas readings, drill stem tests, casing shoe points	Vertical seismic profile	Well tops, cutting descriptions
Well C	Drilling mud weight (log headers), gas readings, casing shoe points	Sonic log	Well tops, cutting descriptions
Well D	Drilling mud weight (log headers), gas readings, casing shoe points	Vertical seismic profile	Well tops, cutting descriptions
Wells B1–B15	Not applicable	Not applicable	Well tops, cutting descriptions

points for the 3D basin model. An additional set of 14 wells plus one well approximately 7 km WNW outside of the study area were used to constrain extent and thickness of the stratigraphic units included in the 3D basin model (Fig. 4). Table 1 summarizes the used well data of this study.

Methodology—velocity-based pore pressure analysis

For the velocity-based pore pressure analysis of the four calibration wells A, B, C and D, available sonic log and vertical seismic profile (VSP) data were used to estimate shale pore pressure. Thereby, the workflow strictly followed the methodology and normal compaction trend developed by Drews et al. (2018), who used a combination of an Athy-porosity law (Athy 1930) modified for effective stress (c.f. Heppard et al. 1998; Hubbert and Rubey 1959; Scott and Thomsen 1993) and a porosity–velocity transform for shales (Issler 1992; Raiga-Clemenceau et al. 1988) to constrain a normal compaction trend for shales from wells with normally pressured shale sections in the North Alpine Foreland Basin in SE Germany. In combination with the Eaton pressure transform for seismic velocity (Eaton 1972, 1975), the normal compaction trend can be used to estimate pore pressure in the North Alpine Foreland Basin in SE Germany.

The described method requires an estimate of the vertical stress σ_v. Sufficient density data are neither available for the calibration wells, nor for the Geretsried GEN-1 well. Thus, the velocity–density transform of Gardner et al. (1974) was applied in those cases in which vertical seismic profile data were available for the entire well. Otherwise, an Athy-type effective stress–porosity relationship with the parameters defined by Drews et al. (2018) was used. In this study, pore pressures and subsurface stresses are usually presented as pressure/stress gradients in equivalent mud weight (EMW) with the density unit g/cm^3, which is calculated as follows.

$$\mathrm{EMW} = \frac{\mathrm{PP}}{g * \mathrm{TVD}}, \quad (1)$$

Table 2 Depth difference between actual well tops of wells within the AOI and modeled stratigraphic tops

	Well A (m)	Well B (m)	Well C (m)	Well D (m)	B2 (m)	B4 (m)	B7 (m)	B12 (m)
Quarternary	0	9	1	33	− 2	1	4	− 5
OSM	0	12	10	− 7	1	− 1	7	− 2
Burdigalian	− 3	23	− 14	17	2	− 10	− 1	− 5
Aquitanian	− 6	12	− 36	34	− 2	− 6	− 12	5
Chattian	1	7	− 17	20	− 5	− 6	− 11	1
Rupelian	4	6	− 21	70	6	− 4	19	− 9
Sannoisian	13	− 24	− 7	18	− 1	n/a	1	26
Eocene	13	− 25	− 10	30	n/a	n/a	[illegible]	27
U. Cretaceous	n/a	− 26	− 12	35	n/a	n/a	1	22
L. Cretaceous	14	− 27	n/a	51	− 1	n/a	[illegible]	14
Jurassic	11	− 30	n/a	56	5	n/a	n/a	34

where PP is the pore pressure in kPa, g is the Earth's gravitational acceleration at 9.81 m/s^2 and TVD is the true vertical depth in m, referenced to the ground level of the drill site. In Eq. 1, PP can also be substituted by any stress parameter to represent stress in equivalent mud weight.

Methodology—3D basin modeling

A simple 3D basin model has been set up using the PetroMod© Modeling Software 2016.2 to investigate (a) the subregional pore pressure distribution, (b) the impact of presence and distribution of stratigraphic units (e.g. erosion of Upper Cretaceous strata in the NW of the study area) and (c) the predictability of overpressure in the North Alpine Foreland Basin in SE Germany, using simplified basin models.

Geological and geometric constraints

The model is purely based on stratigraphic well tops from well reports of all 20 wells, hence does not include any structural elements such as faults. The individual horizons have been generated on the basis of interpolation of thicknesses of the respective stratigraphic units. In the area of interest (AOI), the resulting maximum difference between actual present-day well tops and modeled stratigraphic tops at the individual well location does not exceed 70 m for the top Rupelian (Table 2) below the Chattian, which is the thickest stratigraphic unit (average thickness of 1200 m in the AOI) and, therefore, associated with the highest potential deviation. Facies variations within individual stratigraphic units have not been included in the basin model to keep the degrees of freedom to a minimum. Therefore, the model results represent general pore pressure trends and cannot reflect pressure perturbations due to structural or facies-related heterogeneities.

A horizontal cell size of 1 km × 1 km was used. The basin model comprises 11 layers and the number of sublayers has been set such that the vertical cell size does not exceed 500 m (Table 3). The extent of the basin model is identical to the map of Fig. 4a, resulting in an 80 km × 50 km grid. Geologic ages (c.f. Table 3) for the Cenozoic section have been assigned according to Kuhlemann and Kempf (2002), except for the geological ages of the Lattorf/Sannoisian and Eocene, which have been derived from Zweigel (1998). Since

Table 3 Age, lithology, porosity and permeability models for stratigraphic units used in the 3D basin model

Stratigraphy (layer name)	Age (Ma)	Number of sublayers	Lithology	Porosity model	Permeability model
Quaternary	0	1	Sandstone	Hantschel and Kauerauf (2009), "Sandstone (typical)"	Hantschel and Kauerauf (2009); "Sandstone (typical)"
Upper freshwater Molasse (OSM)	6.7	2	Sandstone	Hantschel and Kauerauf (2009); "Sandstone (clay rich)"	Hantschel and Kauerauf (2009); "Sandstone (clay rich)"
Burdigalian	16.4	2	Sandstone	Hantschel and Kauerauf (2009); "Sandstone (clay rich)"	Hantschel and Kauerauf (2009); "Sandstone (clay rich)"
Aquitanian	20.5	3	Sandstone	Hantschel and Kauerauf (2009); "Sandstone (clay rich)"	Hantschel and Kauerauf (2009); "Sandstone (clay rich)"
Chattian	23.8	5	Shale	Drews et al. (2018)	Yang and Aplin (2010)
Rupelian	28.5	3	Shale	Drews et al. (2018)	Yang and Aplin (2010)
Sannoisian	34	1	Organic-rich shale	Drews et al. (2018)	Yang and Aplin (2010); Eq. 2
Eocene	35.4	1	Limestone	Hantschel and Kauerauf (2009); "Limestone (chalk, typical)"	Hantschel and Kauerauf (2009); "Limestone (chalk, typical)"
Upper Cretaceous	66	1	Organic-rich shale	Drews et al. (2018)	Yang and Aplin (2010); Eq. 2
Lower Cretaceous	100.5	1	Limestone	Hantschel and Kauerauf (2009); "Limestone (ooid grainstone)"	Hantschel and Kauerauf (2009); "Limestone (ooid grainstone)"
Jurassic	145	2	Limestone	Hantschel and Kauerauf (2009); "Limestone (ooid grainstone)"	Hantschel and Kauerauf (2009); "Limestone (ooid grainstone)"

the Cenozoic basin subsidence put the underlying Mesozoic strata most likely to their maximum burial depth, Paleocene and Eocene erosion has only been modeled as stratigraphic pinch-outs of the eroded strata (Fig. 4). Accordingly, geologic ages for the underlying Mesozoic strata were simply derived from the International Chronostratigraphic Chart (Cohen et al. 2013). Thus, the Mesozoic section of the 3D basin model of this study should be seen as a pre-existing basement section, while the actual basin modeling process starts with the Cenozoic basin fill.

Lithological and petrophysical constraints

Since no lateral facies variations have been modeled, a single lithology, compaction and permeability model has been assigned to each stratigraphic unit (Table 3).

Except for the shale-rich stratigraphic units (Chattian, Rupelian, Lattorf/Sannoisian and Upper Cretaceous), porosity and permeability (Table 3) have been modeled using Athy's depth–porosity relationship (Athy 1930) and a three-point porosity–permeability relationship, respectively, with parameters for both porosity and permeability models provided by Hantschel and Kauerauf (2009). Thereby, the Neogene (Miocene and younger) sections have been modeled as permeable siliciclastic sands, while the Lower Cretaceous and Upper Jurassic have been modeled as a nearly uncompressible limestone to mimic the high permeability present in these carbonates even at depths > 4000 m (Przybycin et al. 2017). The Eocene Lithothamnium Limestone has been modeled with chalk properties to represent a fast compacting limestone.

Chattian, Rupelian, Lattorf/Sannoisian and Upper Cretaceous have been modeled as shale-rich units, which are important for overpressure generation. Thereby, shale compaction (porosity as a function of effective stress) has been modeled with the same porosity trend as used for constraining the normal compaction trend of the velocity-based analysis (c.f. Drews et al. 2018). Shale permeabilities have been determined by a pore pressure calibration procedure. Thereby, the clay content-dependent porosity–permeability relationship developed by Yang and Aplin (2010) has been employed. Both the relatively thin Lattorf/Sannoisian and Upper Cretaceous shales are known to comprise the maxima in overpressure in the North Alpine Foreland Basin in SE Germany (Drews et al. 2018), suggesting very low permeability of these units. Since, at least the Lattorf/Sannoisian shale is known to be organic rich (Bachmann et al. 1987), two-phase permeability reduction offers a possible explanation for the low permeability of the Lattorf/Sannoisian and possibly Upper Cretaceous shales. Laboratory studies demonstrated that two-phase permeability of mudrocks can be reduced by > 2 orders of magnitudes compared to single-phase permeabilities (Busch and Amann-Hildenbrand 2013). To represent decreased relative water permeability due to hydrocarbon generation within these shales, permeabilities of Lattorf/Sannoisian and Upper Cretaceous shales have also been modeled using a newly developed temperature–permeability relationship.

$$K_T = \log 10\left(K_{\mathrm{hcg}}\right) * \ln\left(\frac{T}{T_{\mathrm{hcg}}}\right), \quad (2)$$

where K_T is the temperature-dependent permeability in m^2, T is the actual subsurface temperature in °C, K_{hcg} is the permeability in m^2 at T_{hcg}, which is the temperature in °C at which hydrocarbon generation is sufficient to generate a hydrocarbon saturated shale with significantly reduced water-permeability. This can be expected to start with the onset of catagenesis at temperatures between 50 and 150 °C (e.g., Bjørlykke 2015). Figure 5 shows a comparison between permeability calculations based on Eq. 2, calculations of vertical permeability by Yang and Aplin (2010) for 40%, 70% and 90% clay content and calculations of effective permeability by applying the two-phase permeability model of Busch and Amann-Hildenbrand (2013) to the vertical permeability based on Yang and Aplin (2010) for 70% clay content. In this study, the proposed temperature-dependent permeability model (Eq. 2) is calibrated such that below temperatures of 50 °C, it yields lower permeabilities than the low-permeability configuration (90% clay content) of the model by Yang and Aplin (2010) (Fig. 5). Thereby, K_{hcg} and T_{hcg} are fixed to 10^{-22} m^2 and 80 °C, respectively.

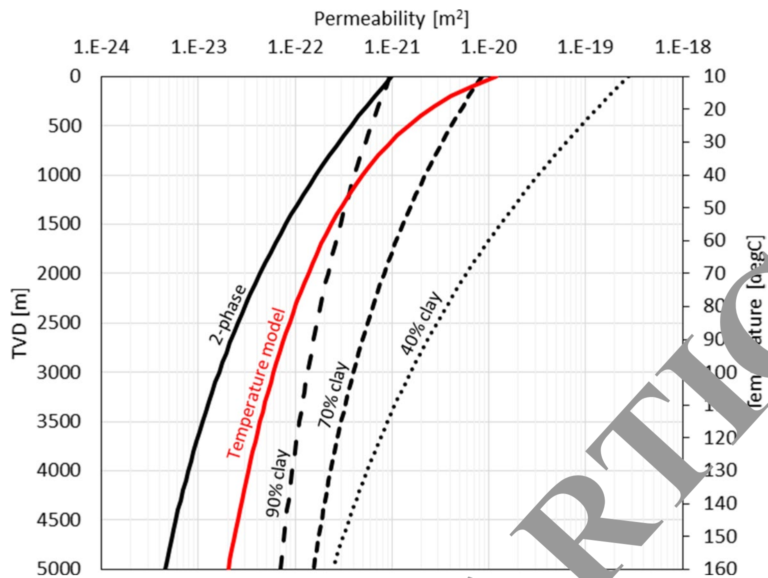

Fig. 5 Shale-permeability models used in this study in comparison to the two-phase model by Busch and Amann-Hildenbrand (2013). Depth and temperature are connected assuming a geothermal gradient of 30 °C/km and a surface temperature of 10 °C. The dotted, and dashed black lines represent the porosity–permeability relationships from Yang and Aplin (2010) for 40%, 70% and 90% clay content, respectively. Porosity has been modeled using the porosity function of Drews et al. (2018) also used in this study. The temperature-dependent permeability model developed in this study is represented by the solid red line. The two-phase permeability model (solid black line) derived from application of the model of Busch and Amann-Hildenbrand (2013) to the porosity–permeability relationship of Yang and Aplin (2010) for 70% clay content

Boundary conditions

The Upper Jurassic carbonate aquifer (Malm) is also known to be at sub-hydrostatic to hydrostatic pressure conditions (Drews et al. 2018; Lemcke 1976). Therefore, a permanent hydrostatic pressure boundary condition (referenced to sea level) has been set for the Jurassic. For the modeled geologic history of the study area (200 Ma to present day), a constant surface temperature of 10 °C has been applied. The basal heat flux (BHF) has been set to 53 mW/m² which is in concordance with previous studies in the North Alpine Foreland Basin (Osternhuber et al. 2014). Since only very little information is known about absolute paleo-sea level values and since water depth changes have no impact on effective stress, and thus present-day pore pressure, paleo-water depths were not included (zero water depth assumed for all modeled stratigraphic events). However, a sensitivity study has been performed to test the influence of extreme values for basal heat flux, paleo-water depth and surface temperature.

Simulation and pore pressure calibration

Temperature and pressure evolution through time has been simulated using the PetroMod© Simulation Software 2016.2 without considering hydrocarbon generation and migration (c.f. Hantschel and Kauerauf 2009).

The 3D basin model has been calibrated to the pore pressure gradient profiles of the wells A, B, C and D. To do so, the permeability models of the Chattian, Rupelian, Lattorf/Sannoisian and Upper Cretaceous shales have been varied, by either applying a different clay content (40%, 70% or 90%) to the porosity–permeability relationship by Yang and Aplin (2010) or using the temperature-dependent permeability function developed in this study (c.f. Eq. 2). From litho-stratigraphic analysis (Kuhlemann and Kempf 2002) and known overpressure magnitudes (Drews et al. 2018), it follows that the Lattorf/Sannoisian and Upper Cretaceous must comprise higher clay and/or organic content, and therefore lower permeabilities than the shales of the Chattian and Rupelian. From cutting descriptions also follows, that the Chattian generally comprises more sandy units than the Rupelian, and is therefore likely more permeable than the Rupelian. Incorporating these relationships by the following rule allows for significant reduction of possible permeability model combinations.

$$K_{\mathrm{Ch}} \leq K_{\mathrm{Ru}} < K_T \quad \text{and} \quad K_{\mathrm{Ru}} \leq K_{\mathrm{LS}} \quad \text{and} \quad K_{\mathrm{Ru}} \leq K_{\mathrm{UC}}, \tag{3}$$

where K_{Ch}, K_{Ru}, K_{LS}, K_{UC} are the permeabilities at a given depth of the Chattian, Rupelian, Lattorf/Sannoisian and Upper Cretaceous shales, respectively. K_T is the temperature-dependent permeability defined in Eq. 2.

The resulting models are then tested against the average deviation from the maximum recorded pore pressure gradients in EMW at the calibration wells A–D. Hereby, we define ± 0.15 g/cm^3 as an acceptable range of average deviation, which matches the uncertainty range of velocity-based pore pressure estimates (Drews et al. 2018) and still allows for quick well control intervention in case of drilling problems. The models satisfying this average uncertainty range are then investigated further for each calibration well to find the best calibration. The calibrated basin model then represents the base case model, which is finally tested against the pore pressure profile at the Geretsried GEN-1 well location.

Results

Pore pressure calibration of the 3D basin model

As an initial step, the average deviation of the modeled pore pressure gradient EMW in g/cm^3 from the maximum pore pressure gradients of the calibration wells has been investigated. Therein, the impact of the Chattian and Rupelian was tested first, while the Lattorf/Sannoisian and Upper Cretaceous are set to the minimum permeability, which is given by the temperature-dependent permeability model (K_T; Eq. 2). From this, it quickly follows that the permeability model of Yang and Aplin (2010) applied to both Chattian and Rupelian shales requires a minimum clay content of 70%, which reduces the number of models for the calibration routine. The upper part of Table 4 (models 1–19) summarizes the modeling rationale, simulated models for the pore pressure calibration and average pressure gradient deviations.

Only considering the average pressure gradient deviation, the temperature-dependent permeability model (K_T; Eq. 2) must be applied to either the Lattorf/Sannoisian or Upper Cretaceous shales to build up sufficient overpressure, except for a configuration of 90% clay content for all shale-rich units (model 17; Table 4). In the case of the Lattorf/Sannoisian or Upper Cretaceous being modeled with the temperature-dependent permeability model (K_T; Eq. 2), the basin model yields overly high average overpressure when permeability of Chattian and Rupelian shales are both modeled after Yang and Aplin (2010) and 90% clay content (models 3, 18, 19; Table 4).

Table 4 Pore pressure calibration table and modeling rationale

#	Clay content of Yang and Aplin (2010), or K_T (Eq. 2)				Average deviation (g/cm^3)	Comment
	Chattian	Rupelian	Lat./San.	U. Cret.		
1	40%	40%	K_T	K_T	– 0.48	Too low → Chattian or Rupelian clay content > 40%
2	70%	70%	K_T	K_T	0.01	Good
3	90%	90%	K_T	K_T	0.34	Too high
4	40%	70%	K_T	K_T	– 0.41	Too low → Chattian and Rupelian clay content > 40%
Decision: Chattian and Rupelian clay content ≥ 70%						
5	70%	70%	70%	70%	– 0.37	Too low
6	70%	70%	70%	90%	– 0.29	Too low
7	70%	70%	70%	K_T	– 0.09	Good
8	70%	70%	90%	70%	– 0.34	Too low
9	70%	70%	90%	90%	– 0.26	Too low
10	70%	70%	90%	K_T	– 0.08	Good
11	70%	70%	K_T	70%	– 0.11	Good
12	70%	70%	K_T	90%	– 0.08	Good
13	70%	90%	90%	90%	– 0.20	Too low
14	70%	90%	90%	K_T	0.01	Good
15	70%	90%	K_T	90%	0.03	Good
16	70%	90%	K_T	K_T	[illegible]	Good
17	90%	90%	90%	90%	– 0.01	Good
18	90%	90%	90%	K_T	0.16	Too high
19	90%	90%	K_T	90%	0.27	Too high
Sensitivity study → Lat./San. and/or U. Cret. clay content = 40%						
20	90%	90%	40%	40%	– 0.17	Too low → Lat./San. or U. Cret. clay content > 40%
21	90%	90%	40%	K_T	0.12	Good
22	90%	90%	K_T	40%	0.21	Too high
23	70%	70%	K_T	40%	– 0.13	Good
24	70%	90%	40%	K_T	– 0.02	Good
25	70%	70%	40%	K_T	– 0.10	Good

Additional models have been run to test the impact of both the Lattorf/Sannoisian and Upper Cretaceous on overpressure build up in the study area (models 20–25; Table 4). Even, if the shale permeability of the Chattian and Rupelian is modeled with a low-permeability model (Yang and Aplin 2010; 90% clay content), the basin model yields overly low average pore pressures for higher permeability (Yang and Aplin 2010; 40% clay content) within Lattorf/Sannoisian and Upper Cretaceous shales (model 20; Table 4). The results of models 20–25 further demonstrate that a very-low-permeability unit (represented by the temperature-dependent permeability model K_T; Eq. 2) in the Lattorf/Sannoisian or Upper Cretaceous is required to build up sufficient overpressure on an average basis.

The total of 25 models yielded 13 models with an acceptable average deviation from the maximum recorded pore pressure gradients at the calibration wells A–D (Table 4). Further investigation of these 13 models for each calibration well shows that application of 90% clay content to the permeability model of Yang and Aplin (2010)

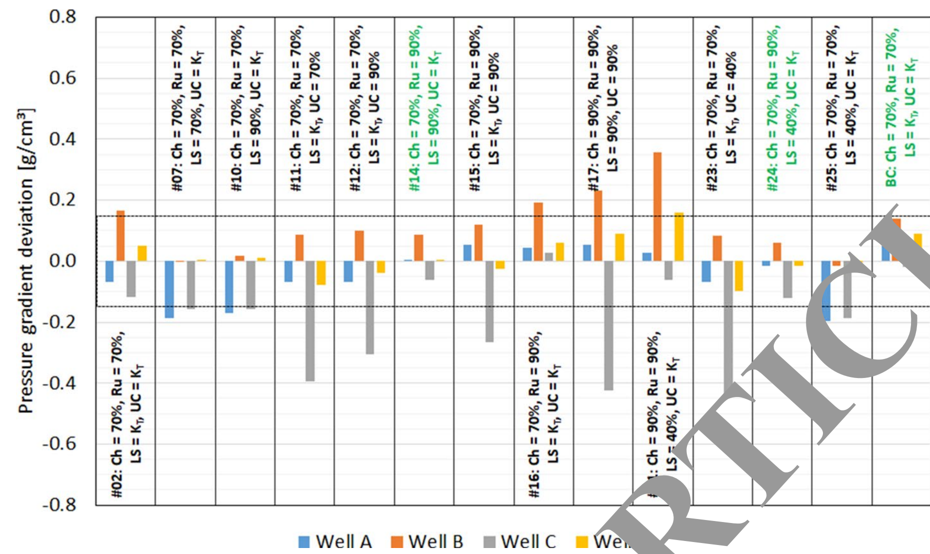

Fig. 6 Calibration well-specific deviation from the maximum pore pressure gradient of the average best fit basin models. For each model the used clay content (40%, 70% and 90%) of the permeability model from Yang and Aplin (2010) or the temperature-dependent permeability model (K_T; c.f. Equation 2) of the Chattian (Ch), Rupelian (Ru), Lattorf/Sannoisian (LS) and Upper Cretaceous (UC) are specified. The black-dotted box indicates the acceptable pressure gradient deviation of 0.15 g/cm^3. The numbers mark the model number used in Table 4. Model descriptions highlighted in green indicate models which yielded acceptable pore pressure deviations at the calibration Wells A–D

for Chattian shales results in an unacceptable overprediction of pore pressure at Well B (Fig. 6). The calibration results also show that the maximum pore pressure gradient at Well C can only be reached in an acceptable range, if the Upper Cretaceous is modeled with the temperature-dependent permeability model (K_T; Eq. 2) developed in this study (Fig. 6). Only two models satisfy the maximum pore pressure gradient deviation range of ± 0.15 g/cm^3 in EMW (models 14 and 24; Fig. 6). However, in model 24, the Lattorf/Sannoisian shale permeability is represented with the highest permeability (Yang and Aplin 2010; 40% clay content), which contradicts the stratigraphic permeability relationship given by Eq. 3. Also, velocity-based pore pressure analyses of Well C in this study (Fig. 7) further indicate that the Lattorf/Sannoisian can comprise very high overpressure and, therefore, very low permeabilities. Model 14, however, provides a reasonable geological representation of permeability distributions amongst the Chattian, Rupelian, Lattorf/Sannoisian and Upper Cretaceous shales. Nevertheless, the resulting pore pressure profiles at the locations of calibration wells A–D yield a slight overprediction in the Chattian and Rupelian and underrepresentation of the Lattorf/Sannoisian overpressure (Fig. 7). In contrast to model 14, the final calibrated model (base case; Fig. 6), therefore, comprises slightly higher Chattian shale permeabilities (Yang and Aplin 2010; 67% clay content) and the very low permeability-yielding temperature-dependent model (K_T; Eq. 2) for the Lattorf/Sannoisian. Especially, the latter appears to be geologically more realistic, since the Lattorf/Sannoisian fish shale has been identified as an important source rock before (Bachmann et al. 1987).

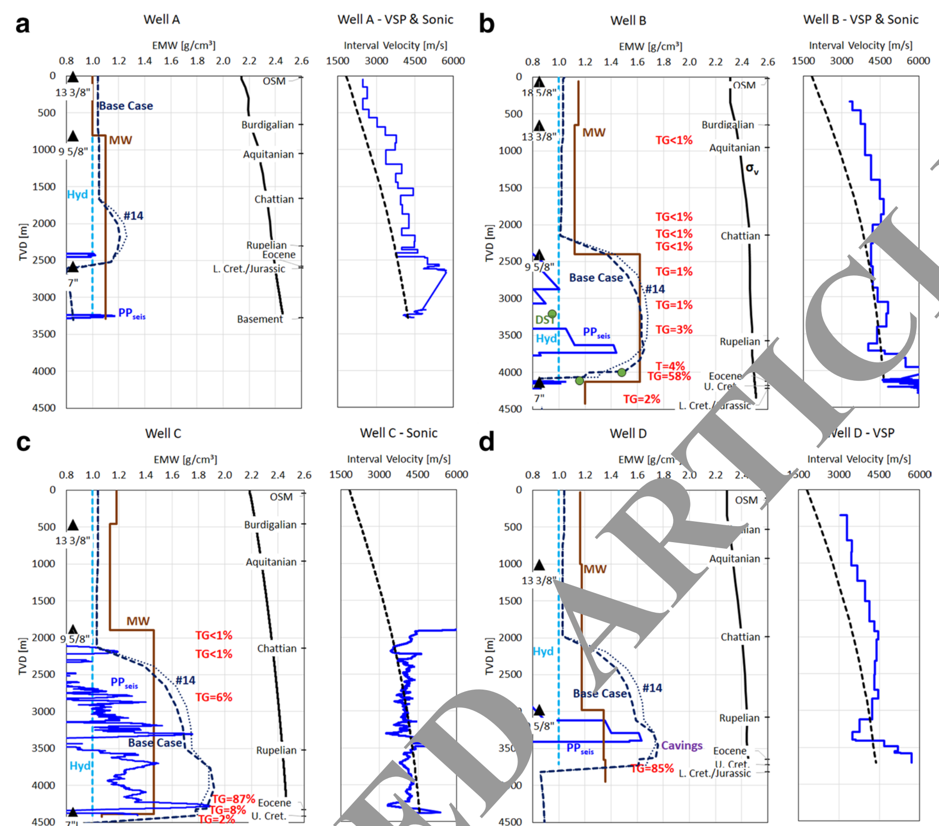

Fig. 7 Pore pressure overview and velocity data of the calibration wells. Depth in true vertical depth (TVD) from ground level, pressure and stress in equivalent mud weight (EMW) in g/cm^3. **a**–**d** also show casing shoe depths (black triangles), drilling mud weight MW (brown line), hydrostatic pressure Hyd (dashed light blue line), estimated pore pressure from VSP or sonic data PP_{seis} (blue line), estimated pore pressure from the base case 3D basin model *base case* (dashed dark blue line) and model #14 (dotted dark blue line), vertical stress σ_v (solid black line), total gas readings TG (red annotations) and stratigraphic tops (black annotations). **a** Overview of Well A. Total gas data were not available. **b** Overview of Well B. The green dots represent drill stem test pressure data. **c** Overview of Well C. **d** Overview of Well D. Pressure cavings are annotated in purple

Sensitivity analysis of basal heat flux, surface temperature and paleo-water depth

Since the permeability function of Lattorf/Sannoisian and Upper Cretaceous shales of the base case model is temperature dependent, a sensitivity study was run. Based on the base case model, models with basal heat flux values of 30 mW/m^2 and 70 mW/m^2, a constant surface temperature of 30 °C and a paleo-water depth of 1000 m were run. According to the algorithm of Wygrala (1989), 30 °C as maximum surface water interface temperature represents the maximum for the latitude of the North Alpine Foreland Basin in SE Germany. The sensitivity study shows that the impact of these parameters is fairly minimal on the estimated pressures at the Geretsried GEN-1 well location (Fig. 8a). Variation of these parameters results in stay within the acceptable uncertainty range of ± 0.15 g/cm^3 in equivalent mud weight. Thereby, a comparison between the modeled temperature profiles and the measured bottom-hole temperature at the Geretsried GEN-1 well location and all other wells in the AOI indicates that the values used for basal heat flux (53 mW/m^2) and average surface temperature (10 °C) capture

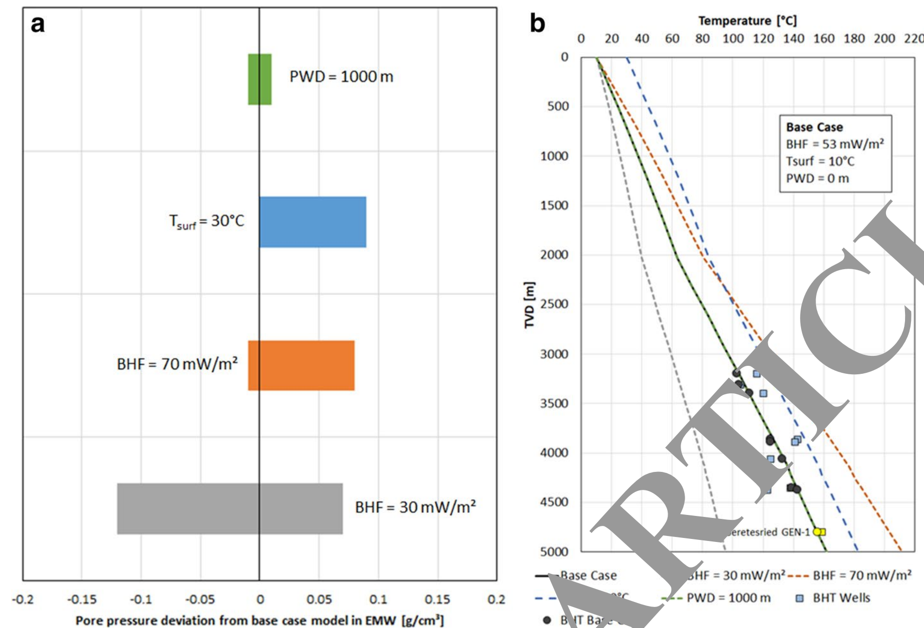

Fig. 8 Results of sensitivity study of base case model. **a** Minimum and maximum pore pressure gradient deviation from base case model at the Geretsried GEN-1 well location using different parameters for paleo-water depth (PWD), surface temperature (T_{surf}) and basal heat flux (BHF). The black vertical line represents the base case model with PWD = 0 m, T_{surf} = 10 °C and BHF = 53 mW/m^2. **b** Modeled temperature profiles at the Geretsried GEN-1 drill site. The black-dashed line shows the modeled present-day temperature profile at the Geretsried GEN-1 drill site using the base case parameters. The gray-dashed line and red-dashed line represent the modeled temperature profiles for a basal heat flux of 30 mW/m^2 and 70 mW/m^2, respectively. The blue-dashed line marks the modeled temperature profile for a constant temperature profile of 30 °C and the green-dashed line overlying the base case line shows that a change in paleo-water depth to 1000 m has no impact on the modeled temperature profile. The squares represent the measured bottom-hole temperatures in the AOI (light blue filling) and at the Geretsried GEN-1 drill site (yellow filling), while the dots represent the modeled bottom-hole temperatures in the AOI (black fillings) and at the Geretsried GEN-1 drill site (yellow filling)

the overall temperature trend in the area (Fig. 8b). Nevertheless, it should be pointed out that it is not within the scope of this study to forecast subsurface temperatures or geothermal gradients. As expected, the paleo-water depth has no impact on present-day pore pressure magnitudes (Fig. 8a), since effective stress is independent of water depth.

Pore pressure blind test at the Geretsried GEN-1 well location

The 1D extraction of the base case basin model matches the maximum pore pressures in the lower Chattian and Rupelian within ± 0.15 g/cm^3 (Fig. 9). A similar prediction prior to drilling would have avoided the severe kick at 3285 m and other drilling problems in the high pressure zone between 3250 and 4200 m. Hereby, the basin model gives an explanation of the sudden pressure increase at 3285 m: pressure likely builds already in the Chattian shales, although the onset of overpressure might be deeper if the coarser-grained units in the upper Chattian were taken into account (Fig. 9c). Although a medium gas spike of > 5% at ~ 2900 m supports overpressure build up in the Chattian (Fig. 9b), this pressure build up would have been mostly undetected while drilling. Also, a pressure estimate from VSP data does not capture the high pressure in the Baustein Beds. This might be related to different shale composition (either

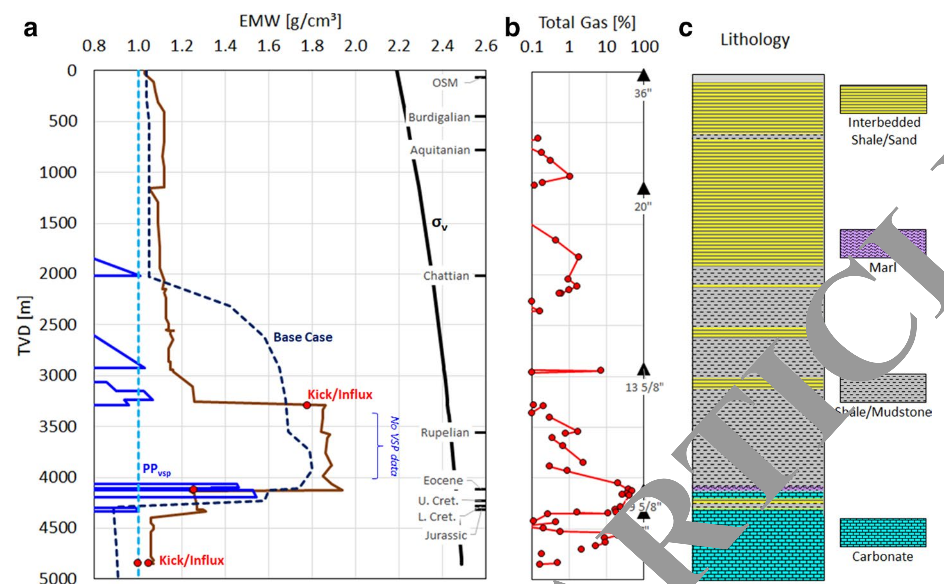

Fig. 9 Pore pressure overview of the Geretsried GEN-1 well. **a** Pore pressure gradient estimate. TVD = true vertical depth; EMW = equivalent mud weight; PP_{vsp} = pore pressure from vertical seismic profile (dark blue-dotted line); base case = pore pressure from base case 3D basin model (dark blue-dashed line); Hyd = hydrostatic/normal pressure (dashed light blue line); MW = drilling mud weight (brown line); kicks/influx = pore pressure estimates from influxes (red dots); σ_v = vertical stress (black line). **b** Total gas readings while drilling on a logarithmic scale in percent (red line and red dots) and casing points (black triangles). **c** Simplified lithological column

coarser-grained or more carbonate-rich) of the Chattian compared to the Rupelian, Lattorf/Sannoisian and Upper Cretaceous, requiring a different normal compaction trend for the Chattian to estimate pore pressure from seismic velocities.

The additional influx at 4115 m recorded through high gas and subsequent drilling mud weight increase to a maximum of 1.94 g/cm^3 is also reflected through the basin model extraction by a pore pressure increase in the Rupelian-to-Lattorf/Sannoisian. However, the maximum pressure predicted by the basin model is just slightly above an MW of 1.8 g/cm^3, but still within the set pressure gradient uncertainty of ±0.1[illegible] g/cm^3. Unfortunately, no VSP data were available for the Rupelian section to further validate the actual pore pressure.

Within the Eocene, the basin model matches predicted shale pore pressure from VSP data. In this section, shale pore pressure is likely higher as pressure of the gas-bearing sands of the lower Eocene section, which indicates that the pore pressure regression towards the Jurassic is already starting in the Eocene. Accordingly, in the Upper Cretaceous, pressures are finally decreasing to the slightly above hydrostatic conditions in the carbonates of the Lower Cretaceous and Jurassic. This decline is also represented in the 1D extraction of the base case basin model (Fig. 9a).

Discussion

The results of this study demonstrate that pore pressure can be predicted within an acceptable uncertainty using simple 3D basin models calibrated to a minimum number of wells. In this study, four calibration wells were sufficient to predict the pore pressure profile at the Geretsried GEN-1 well location. The pore pressure calibration process yielded some interesting insights on the hydraulic controls and mechanisms possibly driving overpressure generation and preservation in the North Alpine Foreland Basin in SE Germany:

The 3D basin model demonstrates that for all shale-rich stratigraphic units, very low permeabilities in the range of 10^{-23}–10^{-20} m^2 are required to build up overpressure through disequilibrium compaction against the hydraulic pull of the under- to normally pressured Jurassic aquifer. However, such permeabilities are not unusual for clay-rich and/or organic-rich shales (Busch and Amann-Hildenbrand 2013; Hildenbrand et al. 2002; Kwon et al. 2001; Lee and Deming 2002; Luffel et al. 1993; Yang and Aplin 2007, 2010). Especially, when considering capillary sealing due to primary kerogen–hydrocarbon conversion, the resulting two-phase permeability can be reduced by up to two orders of magnitudes (Busch and Amann-Hildenbrand 2013), which might well be the case for both Lattorf/Sannoisian and Upper Cretaceous shales. A similar effect has been postulated for the Anadarko Basin, southwestern Oklahoma (Lee and Deming 2002). In this study, we mimic this effect by a continuous temperature-dependent permeability function (Eq. 2). However, a sudden decrease at the exact onset of catagenesis is also a possible scenario. Nevertheless, disequilibrium compaction (eventually enhanced by capillary sealing in organic material) due to retarded water expulsion over sedimentation and burial rates is likely the dominating mechanism for overpressure generation in the North Alpine Foreland Basin in SE Germany, which confirms hypotheses of previous studies (Drews et al. 2018; Müller and Nieberding 1996; Müller et al. 1988).

The pore pressure calibration has also shown that the presence of a very low permeability (< 10^{-22} m^2) Upper Cretaceous section is important to maintain overpressure against the Upper Jurassic hydraulic pull—in particular, at the location of calibration Well C. This is also supported by the fact that overpressure is not present at the Well A location, where the Upper Cretaceous is missing due to erosion. However, at the location of Well A, Chattian, Rupelian and Lattorf/Sannoisian shales have just reached a burial depth (1500–2500 m) where overpressure starts to build up in the North Alpine Foreland Basin in SE Germany (Drews et al. 2018). Also, maximum sedimentation rates (not decompacted) are also significant lower at the Well A location (~ 180 m/Ma; Fig. 10) compared to wells B, C, and D (~ 350 m/Ma; Fig. 10). Thereby, sedimentation rates derived from the overpressured wells B–D are even higher than previously reported sedimentation rates (Allen and Allen 2013; Zweigel 1998). Nevertheless, the rates at Well A are still high, while at the same time previous more regional studies have clearly shown that overpressure in the Cenozoic section is only present where an overpressured Upper Cretaceous is present (Drews et al. 2018), even at comparable depths and similar thicknesses of Cenozoic stratigraphic units (c.f. Kuhlemann and Kempf 2002). Thereby, the results of the Geretsried GEN-1 well showed that the drainage process and respective pressure regression already start in the Eocene in the study area.

Significant changes of depositional environment of the Chattian, Rupelian, and Lattorf/Sannoisian within the study area (c.f. Fig. 4) have not been reported by respective studies (c.f. Kuhlemann and Kempf 2002). However, a general change from more terrestrial deposits in the WNW towards a pure marine setting in the ESE of the North Alpine Foreland Basin in SE Germany also impacted the regional facies distribution for

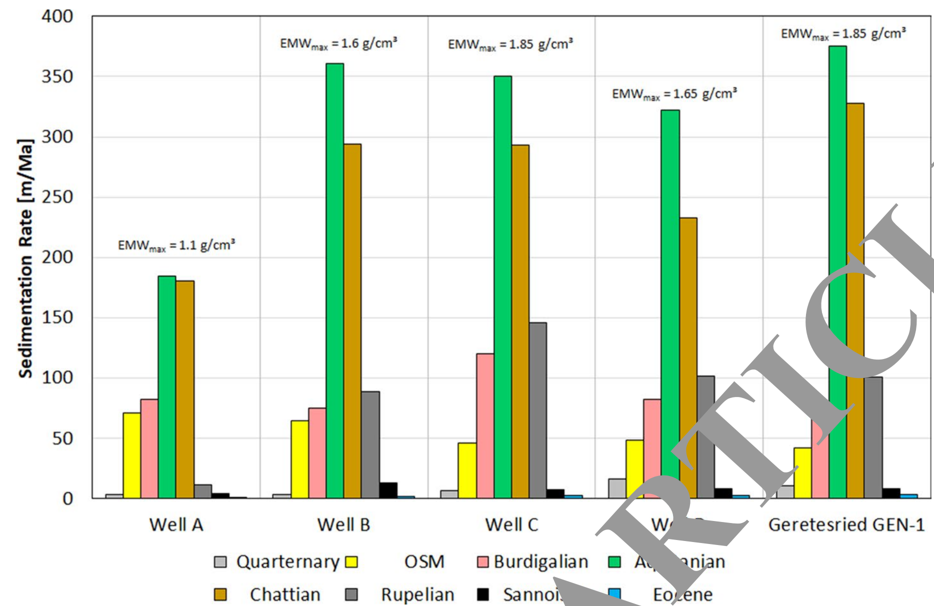

Fig. 10 Non-decompacted sedimentation rates (thickness divided by time interval) for Cenozoic strata from tops of the calibration wells and the Geretsried GEN-1 well. In addition, the maximum observed pore pressure in equivalent mud weight EMW$_{max}$ in g/cm^3 is displayed for each well

the Chattian and Rupelian (c.f. Kuhlemann and Kempf 2002), which is of importance to overpressure generation on the regional scale. Therefore, lower clay content and more permeable shales might be present in the Chattian and Rupelian sections in the west of the study area compared to the east, which might result in local pore pressure deviations from the regional trend and/or impact the velocity-based analysis (e.g., compare velocity-based analyses in the Chattian of Well A to Well C in Fig. 7). To a larger extent, vertical facies/lithological variations within shales likely impact velocity-based pore pressure estimates: estimates of pore pressure from sonic logs and vertical seismic profiles at the calibration Wells A–D show both the highest variability and largest discrepancy to observed (by drilling data) and modeled pressures within the Chattian and Rupelian, which is likely indicating a vertical variability in either grain size (less clay-sized particles) or carbonate content. Both would yield higher velocities and an underestimation of pore pressure from a normal compaction trend, which is also calibrated to the more clay-rich Lattorf/Sannoisian and Upper Cretaceous shales. This is also likely to be the case for the Chattian at the Geretsried GEN-1 well location. Especially in the upper Chattian coarser-grained material has been reported by the cutting descriptions. Since the basin modeling study has clearly shown that pore pressure probably has to build up already in Chattian shales to reach present-day magnitudes, it is, therefore, likely that velocity-based analyses underestimate pore pressure at least within the lower Chattian and upper Rupelian. The water kick in the Baustein Beds (lower Chattian) at the Geretsried GEN-1 well location supports this hypothesis.

The 3D basin model applied in this study does not consider any structural elements, which are abundantly present as normal faults in the entire North Alpine Foreland Basin in SE Germany. However, most of these normal faults only comprise throws on the order of 10–100 m (c.f. von Hartmann et al. 2016). Pore pressure perturbations due to hydrocarbon accumulation against these faults would, therefore, be very small and well within the range of uncertainty defined in this study (±0.15 g/cm^3). Otherwise, faults generating local pressure compartments in the Jurassic aquifer might have an impact on overpressure preservation, if these faults prevented the Jurassic from hydraulic drainage. Also, structural dip and resulting lateral pressure transfer might contribute to unexpected high pore pressure magnitudes as observed in the Baustein Beds at the Geretsried GEN-1 well location. Lateral pressure transfer has been observed in other sedimentary basins with high stratigraphic dip or structural relief (Lupa et al. 2002; Yardley and Swarbrick 2000). Based on the well data used in this study, the stratigraphy equivalent to the Baustein Beds (base Chattian or top Rupelian) is generally dipping towards the south generating a structural relief of ~500 m from the Geretsried GEN-1 location to the southern edge of the study area with an overall structural relief of ~2000 m across the entire study area. However, a study including 3D seismic data would be necessary to quantify the lateral continuity of the Baustein Beds and the possible effect of lateral pressure transfer on pore pressure magnitudes of the Baustein Beds in the greater Geretsried GEN-1 area.

Finally, clay diagenesis as a secondary mechanism of overpressure generation in the study area is feasible for Rupelian, Lattorf/Sannoisian and Upper Cretaceous shales, since these units reach required temperatures in excess of 60 °C, which is the minimum onset temperature for clay diagenesis (cf. Colten-Bradley 1987; Osborne and Swarbrick 1997). Onset of clay diagenesis has been previously reported around 2000–2500 m TVD in the Austrian Molasse Basin and Vienna Basin (Gier 1998, 2000; Gier et al. 2018). However, high-quality density data would be required to test the impact of clay diagenesis on overpressure generation (cf. Hoesni 2004).

Conclusions

Drilling histories and velocity-based pore pressure analyses of the Geretsried GEN-1 well and four calibration wells were integrated with a pore pressure-centric (no hydrocarbon generation simulated) 3D basin model in the North Alpine Foreland Basin in SE Germany for the first time. The results of this study show that pore pressure and, therefore, overpressured zones in the North Alpine Foreland Basin in SE Germany can be predicted using simple 3D basin modeling calibrated to drilling and velocity data-based analyses of a minimum number of wells. This has great impact on future drilling for deep geothermal projects in the North Alpine Foreland Basin in SE Germany, since well design, avoidance of non-productive time and drilling safety critically depend on accurate prediction of subsurface pressures.

Overpressure generation and present-day presence in the North Alpine Foreland Basin in SE Germany critically depend on (a) sufficient sedimentation/burial rates and the presence of low permeability sequences and (b) the presence and absence of low-permeability Upper Cretaceous shales, which act as pressure barrier against the hydraulic pull of the under- to normally pressured Jurassic aquifer. As a consequence, the study also demonstrates the importance of integrating different data sources with a geological model that captures the most important processes and parameters when predicting pore pressure: in this case, spatial variation of sedimentation rates and the presence or absence of low-permeability pressure barriers. Furthermore, due to lithological variability, magnitudes of overpressure in the lower Chattian and upper Rupelian are likely higher than estimated from conventional velocity and drilling data-based methods, if calibrated to a single normal compaction trend.

Finally, the results of this study will have great impact on future studies on the evolution and hydro-mechanical characterization of the North Alpine Foreland Basin in SE Germany, which, for example, is key to understand induced microseismicity associated with injection wells, and the local and regional stress fields.

Authors' contributions

MCD designed the study, conducted the data analysis, interpretation and 3D basin modeling and wrote the manuscript. PH significantly participated in analyzing the well data and in drafting the manuscript. KZ initiated the study and together with HS participated in the writing process of the manuscript. RS and AG completed the data set and were involved in quality control of the Geretsried GEN-1 well analysis. All authors read and approved the final manuscript.

Author details

[1] Geozentrum Nordbayern, Friedrich-Alexander-University (FAU) Erlangen-Nuremberg, Schlossgarten 5, 91054 Erlangen, Germany. [2] Chair of Hydrogeology, Technical University of Munich, Arcisstr. 21, 80333 Munich, Germany. [3] ENEX Power Germany GmbH, Hauptstr. 45-47, 85614 Kirchseon, Germany.

Acknowledgements

First thanks go to Enex Power Germany GmbH for approval to publish data from the Geretsried GEN-1 well. The authors would also like to thank the data owners of all other wells used in this study ENGIE Deutschland AG, ExxonMobil Production Deutschland GmbH, DEA Deutsche Erdoel AG and Wintershall Holding GmbH, represented by the Bundesverband Erdgas, Erdöl und Geoenergie e.V. (BVEG). In addition, the authors would like to thank Schlumberger for providing an academic license for the PetroMod© Modeling and Simulation software and Dr. Oliver Schenk for valuable advice in the topic of basin modeling. Finally, the authors would like to thank three anonymous reviewers for their comments and suggestions, which have greatly helped to improve the structure and readability of the manuscript.

Competing interests

The authors declare that they have no competing interests.

Availability of data and materials

The data that support the findings of this study are available from Enex Power Germany GmbH, ENGIE Deutschland AG, ExxonMobil Production Deutschland GmbH, DEA Deutsche Erdoel AG and Wintershall Holding GmbH, but restrictions apply to the availability of these data, which were used under license for the current study, and so are not publicly available. Data are however available from the authors upon reasonable request and with permission of Enex Power Germany GmbH, ENGIE Deutschland AG, ExxonMobil Production Deutschland GmbH, DEA Deutsche Erdoel AG and Wintershall Holding GmbH.

Ethics approval and consent to participate

This research does not involve any human subjects, human material, or human data.

Funding

This work was funded by the Bavarian State Ministry for Education, Culture, Science and Arts within the framework of the "Geothermal Alliance Bavaria (GAB)" and the German Federal Ministry for Economic Affairs and Energy through the project "Dolomitkluft".

Publisher's Note

Springer Nature remains neutral with regard to jurisdictional claims in published maps and institutional affiliations.

Received: 3 August 2018 Accepted: 25 January 2019
Published online: 04 February 2019

References

Allen PA, Allen JR. Basin analysis: principles and application to petroleum play assessment. 3rd ed. Chichester: Wiley-Blackwell; 2013.

Athy LF. Density, porosity and compaction of sedimentary rocks. AAPG Bull. 1930;14:1–24.

Bachmann GH, Müller M, Weggen K. Evolution of the Molasse basin (Germany, Switzerland). Tectonophysics. 1987;137:77–92. https://doi.org/10.1016/0040-1951(87)90315-5.

Bjørlykke K. Petroleum geoscience: from sedimentary environments to rock physics. 2nd ed. Berlin: Springer; 2015. https://doi.org/10.1007/978-3-642-34132-8.

Bjørlykke K, Jahren J, Aagaard P, Fisher Q. Role of effective permeability distribution in estimating overpressure using basin modelling. Mar Pet Geol. 2010;27:1684–91. https://doi.org/10.1016/j.marpetgeo.2010.05.003.

Bowers GL. Pore pressure estimation from velocity data: accounting for overpressure mechanisms besides undercompaction. SPE Drill Complet. 1995;10:89–95.

Busch A, Amann-Hildenbrand A. Predicting capillarity of mudrocks. Mar Pet Geol. 2013;45:208–23. https://doi.org/10.1016/j.marpetgeo.2013.05.005.
Cohen KM, Finney SC, Gibbard PL, Fan J-X. The ICS international chronostratigraphic chart. Episodes. 2013;36:199–204.
Colton-Bradley VAC. Role of pressure in smectite dehydration—effects on geopressure and smectite-to-illite transition. AAPG Bull. 1987;71:1414–27.
Darby D, Haszeldine RS, Couples GD. Central North Sea overpressures: insights into fluid flow from one- and two-dimensional basin modelling, vol. 141. London: Geological Society of London; 1998. https://doi.org/10.1144/gsl.sp.1998.141.01.06.
Drews MC, Bauer W, Caracciolo L, Stollhofen H. Disequilibrium compaction overpressure in shales of the Bavarian Foreland Molasse Basin: results and geographical distribution from velocity-based analyses. Mar Pet Geol. 2018;92:37–50.
Eaton BA. The effect of overburden stress on geopressure prediction from well logs. J Petrol Technol. 1972;24:929–34. https://doi.org/10.2118/3719-PA.
Eaton BA (1975) The equation for geopressure prediction from well logs. Paper presented at the fall meeting of the SPE of American Institute of Mining, Metallurgical, and Petroleum Engineers, Dallas, Texas, September 28–October 1
Gardner GHF, Gardner LW, Gregory AR. Formation velocity and density—the diagnostic basics for stratigraphic traps. Geophysics. 1974;39:770–80.
Gier S. Burial diagenetic processes and clay mineral formation in the Molasse zone of Upper Austria. Clays Clay Miner. 1998;46:658–69. https://doi.org/10.1346/CCMN.1998.0460606.
Gier S. Clay mineral and organic diagenesis of the lower Oligocene Schoneck Fishshale, western Austrian Molasse basin. Clay Miner. 2000;35:709–17. https://doi.org/10.1180/000985500547151.
Gier S, Worden RH, Krois P. Comparing clay mineral diagenesis in interbedded sandstones and mudstones, Vienna Basin, Austria, vol. 435. London: Geological Society Special Publication; 2018. https://doi.org/10.1144/sp435.9.
Greiner G, Lohr J. Tectonic stresses in the Northern Foreland of the Alpine system—measurements and interpretation. In: Scheidegger AE, editor. Tectonic stresses in the Alpine-Mediterranean Region, vol. 9., Rock Mechanics/Felsmechanik/Mécanique des RochesVienna: Springer; 1980.
Gusterhuber J, Hinsch R, Sachsenhofer RF. Evaluation of hydrocarbon generation and migration in the Molasse fold and thrust belt (Central Eastern Alps, Austria) using structural and thermal basin models. AAPG Bull. 2014;98:253–77. https://doi.org/10.1306/06061312206.
Hantschel T, Kauerauf A. Fundamentals of basin and petroleum systems modeling. Berlin: Springer; 2009.
Heppard PD, Cander HS, Eggertson EB. Abnormal pressure and the occurrence of hydrocarbons in offshore eastern Trinidad, West Indies. Tulsa: AAPG Memoir; 1998. p. 215–46.
Hildenbrand A, Schlömer S, Krooss BM. Gas breakthrough experiments on fine-grained sedimentary rocks. Geofluids. 2002;2:3–23. https://doi.org/10.1046/j.1468-8123.2002.00031.x.
Hoesni MJ. Origins of overpressure in the Malay Basin and its influence on petroleum systems. Durham: Durham University; 2004.
Hubbert MK, Rubey WW. Role of fluid pressure in mechanics of overthrust faulting. Bull Geol Soc Am. 1959;70:115–66.
Issler DR. A new approach to shale compaction and stratigraphic resotration, Beaufort-Mackenzie Basin and Mackenzie Corridor, northern Canada. AAPG Bull. 1992;76:1170–89.
Karlsen DA, Skeie JE. Petroleum migration, faults and overpressure, part I: calibrating basin modelling using petroleum in traps—a review. J Pet Geol. 2006;29:227–56. https://doi.org/10.1111/j.1747-5457.2006.00227.x.
Kuhlemann J, Kempf O. Post-Eocene evolution of the North Alpine Foreland Basin and its response to Alpine tectonics. Sed Geol. 2002;152:45–78. https://doi.org/10.1016/S0037-0738(01)00285-8.
Kwon O, Kronenberg AK, Gangi AF, Johnson B. Permeability of Wilcox shale and its effective pressure law. J Geophys Res Solid Earth. 2001;106:19339–53.
Lee Y, Deming D. Overpressures in the Anadarko basin, southwestern Oklahoma: static or dynamic? AAPG Bull. 2002;86:145–60.
Lemcke K. Übertiefe Grundwässer im süddeutschen Alpenvorland. Bulletin der Vereinigung Schweiz Petroleum-Geologen und Ingenieure. 1976;42:9–18.
Lohr J. Alpine stress documented by anomalous seismic velocities in the Molasse trough. Inter-Union Com Geodyn Sci Rep. 1978;38:69–71.
Luffel DL, Hopkins CW, Schettler Jr PD Matrix permeability measurement of gas productive shales. In: Proceedings—SPE annual technical conference and exhibition; 1993. p. 261–70.
Lupa J, Flemings P, Tennant S. Pressure and trap integrity in the deepwater Gulf of Mexico. Lead Edge. 2002;21:184–7. https://doi.org/10.1190/1.1452610.
Megies T, Wassermann J. Microseismicity observed at a non-pressure-stimulated geothermal power plant. Geothermics. 2014;52:36–049. https://doi.org/10.1016/j.geothermics.2014.01.002.
Mosca F, et al. Pore pressure prediction while drilling: three-dimensional earth model in the Gulf of Mexico. AAPG Bull. 2018;102:545–7. https://doi.org/10.1306/0605171619617050.
Mouchet J-P, Mitchell A. Abnormal pressures while drilling: origins, predictions, detection evaluation. Paris: Editions Technip; 1989.
Mudford BS, Gradstein FM, Katsube TJ, Best ME. Modelling 1D compaction-driven flow in sedimentary basins: a comparison of the Scotian Shelf, North Sea and Gulf Coast, vol. 59. London: Geological Society; 1991. https://doi.org/10.1144/gsl.sp.1991.059.01.05.
Müller M, Nieberding F. Principles of abnormal pressures related to tectonic developments and their implication for drilling activities (Bavarian Alps, Germany). In: Wessely G, Liebl W, editors. Oil and gas in Alpidic Thrusbelts and Basins of Central and Eastern Europe, vol. 5. Amsterdam: EAGE Special Pub; 1996. p. 119–26.
Müller M, Nieberding F, Wanninger A. Tectonic style and pressure distribution at the northern margin of the Alps between Lake Constance and the River Inn. Geol Rundsch. 1988;77:787–96.
Osborne MJ, Swarbrick RE. Mechanisms for generating overpressure in sedimentary basins: a reevaluation. AAPG Bull. 1997;81:1023–41.

Peters KE, Schenk O, Hosford Schelrer A, Wygrala BP, Hantschel T. Basin and petroleum systems modeling. In: Hsu CS, Robinsom PR, editors. Springer handbook of petroleum technology. 2nd ed. Cham: Springer International Publishing; 2017. p. 1238. https://doi.org/10.1007/978-3-319-49347-3.

Przybycin AM, Scheck-Wenderoth M, Schneider M. The origin of deep geothermal anomalies in the German Molasse basin: results from 3D numerical models of coupled fluid flow and heat transport. Geotherm Energy. 2017;1:1. https://doi.org/10.1186/s40517-016-0059-3.

Raiga-Clemenceau J, Martin JP, Nicoletis S. The concept of acoustic formation factor for more accurate porosity determination from sonic transit time data. Log Analyst. 1988;29:54–60.

Reinecker J, Tingay M, Müller B, Heidbach O. Present-day stress orientation in the Molasse basin. Tectonophysics. 2010;482:129–38. https://doi.org/10.1016/j.tecto.2009.07.021.

Rizzi PW. Hochdruckzonenfrüherkennung in Mitteleuropa. Erdoel-Erdgas-Zeitschrift. 1973;89:249–56.

Sargent C, Goulty NR, Cicchino AMP, Ramdhan AM. Budge-fudge method of pore-pressure estimation from wireline logs with application to cretaceous mudstones at haltenbanken. Pet Geosci. 2015;21:219–32. https://doi.org/10.1144/petgeo2014-088.

Satti IA, Ghosh D, Yusoff WIW. 3D predrill pore pressure prediction using basin modeling approach in a field of Malay Basin. Asian J Earth Sci. 2015;8:24–31. https://doi.org/10.3923/ajes.2015.24.31.

Scott DR, Thomsen LA A global algorithm for pore pressure prediction. In: 8th SPE Middle East oil show and conference, Manama, Bahrain, April 3–6 1993. p. 645–54.

Seithel R, Steiner U, Müller B, Hecht C, Kohl T. Local stress anomaly in the Bavarian Molasse basin. Geotherm Energy. 2015. https://doi.org/10.1186/s40517-014-0023-z.

Stober I, Bucher K. Geothermal energy: from theoretical models to exploration and development. New York: Springer; 2013. https://doi.org/10.1007/978-3-642-13352-7.

Swarbrick RE, Osborne MJ. Mechanisms that generate abnormal pressures: an overview. AAPG Memoir; 1998. p. 13–34.

von Hartmann H, Tanner DC, Schumacher S. Initiation and development of normal faults within the German alpine foreland basin: the inconspicuous role of basement structures. Tectonics. 2016;35:1560–74. https://doi.org/10.1002/2016TC004176.

Wygrala BP. Integrated study of an oil field in the southern Po Basin, northern Italy. Cologne: Universität Köln; 1989.

Yang Y, Aplin AC. Permeability and petrophysical properties of 30 natural mudstones. J Geophys Res Solid Earth. 2007. https://doi.org/10.1029/2005jb004243.

Yang Y, Aplin AC. A permeability-porosity relationship for mudstones. Mar Pet Geol. 2010;27:1692–7. https://doi.org/10.1016/j.marpetgeo.2009.07.001.

Yardley GS, Swarbrick RE. Lateral transfer: a source of additional overpressure? Mar Pet Geol. 2000;17:523–37. https://doi.org/10.1016/S0264-8172(00)00007-6.

Ziegler MO, Heidbach O, Reinecker J, Przybycin AM, Scheck-Wenderoth M. A multi-stage 3-D stress field modelling approach exemplified in the Bavarian Molasse basin. Solid Earth. 2016;7:1365–82. https://doi.org/10.5194/se-7-1365-2016.

Zweigel J. Eustatic versus tectonic control on foreland basin fill: sequence stratigraphy, subsidence analysis, stratigraphic modelling, and reservoir modelling applied to the German Molasse basin. Contrib Sedimentary Geol. 1998;20:X–140.